Theoretical and Experimental Investigation on the Rotational Isomerism in α-Fluoroacetophenones

Barbara C. Fiorin,*,† Ernani A. Basso,‡ Cláudio F. Tormena,§ Roberto Rittner,§ and Raymond J. Abraham⊥

Departamento de Química, Universidade Estadual de Ponta Grossa/UEPG, Av. General Carlos Cavalcanti 4748, 84030-900—Ponta Grossa, PR, Brazil, Departamento de Química, Universidade Estadual de Maringá/ UEM, Av. Colombo 5790, 87020-900—Maringá, PR, Brazil, Physical Organic Chemistry Laboratory, Chemistry Institute, State University of Campinas/UNICAMP, Caixa Postal 6154, 13083-862—Campinas, SP, Brazil, and Chemistry Department, University of Liverpool, P. O. Box 147, Liverpool L69 3BX, United Kingdom

Received: September 10, 2008; Revised Manuscript Received: December 20, 2008

The geometries involved in the conformational equilibria of α-fluoroacetophenone, *p*-nitro-α-fluoroacetophenone, and *p*-methoxy-α-fluoroacetophenone were investigated. Theoretical calculations showed that *cis* and *gauche* forms (F−C−C═O) are their most stable conformers and that in the vapor phase the *gauche* conformer is predominant. The three compounds were synthesized, and the conformational behavior in solution was estimated from infrared (IR) and nuclear magnetic resonance (NMR) spectra obtained in solvents of different polarity. Their IR spectra showed one carbonyl absorption for the *cis* and one for the *gauche* conformer, and that the *cis* conformer was preferred in the more polar solvents. $^1J_{CF}$, $^2J_{C(O)F}$, and $^2J_{HF}$ coupling constants were obtained from their NMR spectra, and they also showed a preference for the *cis* conformer when more polar solvents were used. The vapor phase calculations showed a conformational preference for the *gauche* form. However, when the solvent effects were included in the calculations, the results were in complete agreement with the experimental data (NMR and IR), the *cis* conformer being the most stable one.

Introduction

Organic compounds containing a C−F bond are extremely rare in living organisms.[1] The halogens—chlorine, bromine, and even iodine—figure pre-eminently in many of these compounds with ca. 3000 natural products containing these elements reported to date, while fluorine has been identified as a component of only 13 secondary metabolites.[2a]

The first organofluorine compound identified was fluoroacetate, in 1943, as a metabolite of the Southern African plant *Dichapetalum cymosum.* Since its discovery, it has been the most studied, and its biosynthesis in plants was widely investigated.

From a biological standpoint,[2b] there is a considerable interest to understand the nature of the fluorination process to generate completely novel fluorinated products with pharmacological activity, e.g., antibiotics.[2c]

Fluorine substitution in the position α to a carbonyl group of small aliphatic compounds, as well as in α-fluoroaldehydes,[3,4] α-fluoroketones,[5,6] α-fluoroesters,[7,8] and α-fluoroamides,[9,10] gives only two conformers, *cis* and *trans*, except for fluoroamides, where the conformational equilibrium is between *cis* and *gauche* conformers.

The conformational analysis of α-fluoroacetophenone through infrared spectroscopy and molecular-mechanics calculation showed the existence of *cis/gauche* rotational isomerism.[11] Likewise, a study using the proton NMR spectrum of an α-fluoroacetophenone sample dissolved in a nematic liquid crystalline solvent suggested that the *cis* rotamer was the most stable form.[12] Later, Rodríguez et al.[13] studied the potential energy surfaces of acetophenone, α-fluoroacetophenone, and propiophenone. Side-chain fluorine substitution affected the acetophenone structure in a completely different way in comparison to the methyl group. It is interesting to note that the resulting potential energy surfaces for FCH_2−COPh and $MeCH_2$−COPh were noticeably different, but not as much as those reported for FCH_2−COF and $MeCH_2$−COF on the basis of microwave spectroscopy.[13]

In this paper, a computational and experimental study aimed at determining the conformational preferences in some α-fluoroacetophenones involving the F−C−C═O bond is given.

Computational Details

All calculations have been carried out using the GAUSSIAN 03 program package.[14] Potential energy surfaces, at the B3LYP/6-31g(d,p) level, were built by changing the dihedral angle (F−C−C═O) in increments of 10°, ranging from 0° to 180°, with partial geometry optimization at each point. The minimum points were further optimized at the B3LYP/6-311++g(2d,2p) level of theory, with zero-point energy correction (ZPE). The optimized geometries and energies of all rotamers are given in Tables 1 and 2.

Calculated coupling constants were obtained with the same DFT method, but using the EPR-III as the basis set. Electrostatic potential maps[15] were calculated at the B3LYP/6-311++g(2d,2p) level of theory. These maps were plotted using the MOLEKEL program.[16,17] The coupling constants and eletrostatic potential maps were calculated in vapor phase. The solvent effects in

* Corresponding author. E-mail: bcfiorin@uepg.br. Telephone: +55 42 32203731. Fax: +55 42 32203042.
† Universidade Estadual de Ponta Grossa/UEPG.
‡ Universidade Estadual de Maringá/UEM.
§ State University of Campinas/UNICAMP.
⊥ University of Liverpool.

10.1021/jp808048s CCC: $40.75
Published on Web 03/04/2009

TABLE 1: Structural Data, Calculated Energies (*E*), and Dipole Moments (μ) for NFA and FA at the B3LYP/6-311++g(2d,2p) Level in Vapor Phase (298.15 K)

Parameters	NFA		FA	
	cis	***gauche***	***cis***	***gauche***
r (C=O)	1.207	1.213	1.209	1.216
r (C_1–C_3)	1.502	1.496	1.496	1.489
r (C_1–C_7)	1.526	1.526	1.528	1.528
r (C_7–C_8)	1.525	1.526	1.528	1.528
r (C–F)	1.375	1.394	1.378	1.396
r (N–C)	1.479	1.479	----	----
∠ F–C–C	110.6	113.4	110.8	113.6
∠ C_3–C_1=O	121.5	121.3	122.2	121.9
∠ C_7–C_1=O	120.7	117.2	120.2	116.7
∠ O–N–C	117.5	117.5	----	----
ϕ F–C–C=O	0.0	149.3	0.0	145.7
ϕ O=C–C_7–C_8	180.0	162.0	179.9	164.5
ϕ O–N–C–C	0.0	0.5	----	----
E (hartrees)	-688.706868	-688.708406	-484.143686	-484.144763
E_{rel} (kcal.mol^{-1})	0.96	0.00	0.67	0.00
Population (%)	9	91	14	86
μ (Debyes)	2.76	3.74	4.76	1.93

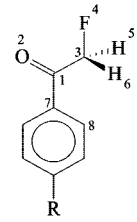

R:

H (FA)

NO_2 (NFA)

TABLE 2: Structural Data, Calculated Energies (*E*), and Dipole Moments (μ) for MFA-*syn* and MFA-*anti* at the B3LYP/6-311++g(2d,2p) Level in Vapor Phase (298.15 K)

Parameters	*MFA*			
	cis-anti	*gauche-anti*	*cis-syn*	*gauche-syn*
r (C=O)	1.211	1.219	1.211	1.219
r (C_1–C_3)	1.487	1.479	1.487	1.480
r (C_1–C_7)	1.530	1.529	1.529	1.529
r (C–F)	1.378	1.398	1.378	1.397
r (C–O_{Me})	1.355	1.355	1.355	1.355
∠ F–C–C	110.8	114.4	110.8	113.8
∠ C_3–C_1=O	122.4	122.2	122.5	122.3
∠ C_7–C_1=O	120.0	115.9	120.0	116.4
∠ C–O–C_{Me}	118.8	118.8	118.8	118.8
ϕ F–C–C=O	0.0	148.3	0.0	145.1
ϕ O=C–C_7–C_8	180.0	167.8	180.0	167.5
ϕ C–C–O– C_{Me}	-180.0	-179.4	180.0	180.0
ϕ C–O–C– H_{Me}	180.0	179.5	180.0	179.9
E (hartrees)	-598.674432	-598.675888	-598.674627	-598.675801
E_{rel} (kcal.mol^{-1})	0.91	0.00	0.79	0.05
Population (%)	5	46	6	43
μ (Debyes)	6.57	3.99	5.49	2.77

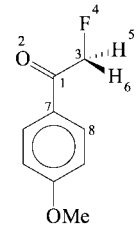

TABLE 3: Experimental Coupling Constants (Hz) for NFA, FA, and MFA

	NFA			FA			MFA		
solvents	$^1J_{CF}$	$^2J_{C(O)F}$	$^2J_{HF}$	$^1J_{CF}$	$^2J_{C(O)F}$	$^2J_{HF}$	$^1J_{CF}$	$^2J_{C(O)F}$	$^2J_{HF}$
$CDCl_3$	184.7	17.0	46.7	182.6	15.5	46.9	182.1	15.5	47.1
CD_2Cl_2	183.1	16.4	46.5	181.1	15.3	46.8	180.3	15.4	46.9
acetone-d_6	179.4	15.7	46.3	178.1	15.1	46.7	177.3	15.2	46.8
CD_3CN	179.0	15.3	46.1	177.3	14.7	46.5	176.5	14.9	46.6
DMSO-d_6	176.8	14.9	45.7	175.6	14.2	46.2	174.8	14.5	46.4

TABLE 4: Experimental ($CDCl_3$) and Calculated (Vapor Phase) Coupling Constants (Hz) at the B3LYP/EPR-III Level

	NFA			FA			MFA		
	exp	*cis*	*gauche*	exp	*cis*	*gauche*	exp	*cis*	*gauche*
$^2J_{C(O)F}$	17.0	12.2	15.6	15.5	12.2	15.3	15.5	12.5	14.8
	46.7	51.8	55.4	46.9	52.3	55.6	47.1	52.4	55.7
$^2J_{HF}$		51.8	53.1		52.3	53.4		52.4	53.5

TABLE 5: Experimental Coupling Constants (Hz) for MFA in CD_2Cl_2 and $CDCl_3$ with Varying Temperature

	CD_2Cl_2			$CDCl_3$		
temp (K)	$^1J_{CF}$	$^2J_{C(O)F}$	$^2J_{HF}$	$^1J_{CF}$	$^2J_{C(O)F}$	$^2J_{HF}$
300	180.10	15.15	46.89	181.68	15.45	47.01
273	179.53	14.95	46.70	181.03	15.16	46.81
253	178.96	14.73	46.60	180.39	14.87	46.66
233	178.37	14.51	46.41	179.46	14.44	46.44
213	178.09	14.44	46.35	—	—	—

TABLE 6: Experimental Coupling Constants (Hz) for NFA in CD_2Cl_2 and $CDCl_3$ with Varying Temperature

	CD_2Cl_2			$CDCl_3$		
temp (K)	$^1J_{CF}$	$^2J_{C(O)F}$	$^2J_{HF}$	$^1J_{CF}$	$^2J_{C(O)F}$	$^2J_{HF}$
300	183.19	16.38	46.51	184.92	16.89	46.77
273	182.83	15.81	46.32	184.56	16.38	46.64
253	182.40	15.52	46.16	184.12	15.95	46.35
233	182.04	15.23	46.00	183.77	15.73	46.18
213	181.54	14.94	45.84	—	—	—

the conformational equilibrium were obtained from optimized vapor phase geometries, at the B3LYP/6-311++g(2d,2p) level, using the polarized continuum model (PCM) in CH_3CN.[18]

Experimental Section

NMR Experiments. ***Solvent Effects.*** The experiments were performed for the three studied compounds. ^1H and ^{13}C NMR spectra were obtained on a Varian Mercury plus BB spectrometer operating at 300.059 MHz for proton and 75.457 MHz for carbon. Spectra were of 0.20 M solutions, with a probe temperature of ca. 28 °C. Typical conditions for proton spectra were 48 transients, spectral width 3000 Hz with 32 k data points and zero-filled 128 k to reach a digital resolution of 0.04 Hz. Decoupled carbon spectra were obtained with 1024 transients, 2 s pulse delay, spectral width 17 000 Hz with 64 k data points and zero-filled 256 k for 0.1 Hz digital resolution. The spectra were all first-order, and the coupling constants, taken directly from them, are shown in Table 3.

Temperature Effects. The experiments were performed for the nitro and methoxy derivatives in CD_2Cl_2 and $CDCl_3$. ^1H and ^{13}C NMR spectra were obtained on a Bruker Avance DPX spectrometer operating at 300.130 MHz for proton and 75.468 MHz for carbon. Spectra were of 0.20 M solutions at probe temperatures of 27, 0, −20, −40, and −60 °C. Typical conditions for proton spectra were 32 k data points and zero-filled 128 k to reach a digital resolution of 0.06 Hz. Decoupled carbon spectra were obtained with 2 s pulse delay, spectral width 18 800 Hz with 64 k data points and zero-filled 256 k for 0.1 Hz digital resolution. The spectra were all first-order, and the coupling constants, taken directly from them, are shown in Tables 5 and 6.

IR Experiments. The carbonyl stretching bands, both in fundamental (1750−1650 cm^{-1}) and in the first overtone regions (3460−3300 cm^{-1}), were recorded on a Bomem FT-IR MB-100 spectrometer, from 0.03 M solutions for all compounds studied, in solvents of varying polarity, using 0.5 mm sodium chloride matched cells for the fundamental region and 1.00 cm quartz matched cells for the overtone region. Deconvolution analyses were performed through the GRAMS program.

Syntheses. ***p-Nitro-α-fluoroacetophenone (NFA).***[19] To a solution of hydrogen fluoride pyridine (6 mL) at −20 °C was slowly added an ethereal solution of diazoacetophenone which was prepared *in situ* from 4-nitrobenzoyl chloride (7.5 mmol) and an excess of diazomethane (∼16.6 mmol). The reaction was allowed to warm to room temperature and was stirred for 14 h. Hydrogen fluoride was removed by treatment of the reaction mixture with aqueous solution of sodium hydrogen carbonate (3%) until neutral. The product was isolated by extraction with hexane (3 × 10 mL), and the solvent was removed under reduced pressure. Purification was carried out over silica gel, eluting with hexane:ethylacetate (20%). Yield of pure product was 2.25 mmol (30%).

^1H NMR (300 MHz, $CDCl_3$): δ (ppm) = 5.52 (d, J = 46.71 Hz, 2H, CH_2F), 8.36 (d, J = 8.7 Hz, 2H, Ar), and 8.10 (d, J =

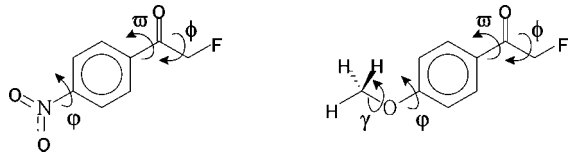

Figure 1. Dihedral angles investigated: ω, φ, ϕ, and γ.

8.7 Hz, 2H, Ar). ^{13}C NMR (75 MHz, $CDCl_3$): δ (ppm) = 84.6 (d, J = 185.05 Hz, CH_2F), 125.0, 130.3, 130.4, 139.3, 194.0 (d, J = 17.0 Hz, CO).

α-Fluoroacetophenone (FA). An ethereal solution of diazomethane (~16.6 mmol) was prepared from commercial Diazald. The flask contents was equipped with nitrogen atmosphere and cooled in an ice bath. Triethylamine (14.2 mmol) and 7.5 mmol of benzoyl chloride in 100 mL of dry ether were added to diazomethane. The mixture was kept in an ice bath for 1 h and then overnight at room temperature. The solvent was removed under reduced pressure. Further purification was reached through successive recrystallizations in pentane and pentane:ether (60:55), yielding 1.3 g (52%) of diazoacetophenone.

To 4 mL of pyridinium poly(hydrogen fluoride) solution at −20 °C was slowly added 1.3 g (7.30 mmol) of diazoacetophenone in dry ether. After being warmed to room temperature and then stirred under nitrogen atmosphere for 11 h, the product was isolated by extraction with 100 mL of pentane. The organic layer was washed with water, 3% aqueous sodium bicarbonate, and water again, and dried over anhydrous magnesium sulfate. Removal of the solvent under reduced pressure and purification by recrystallization from pentane:ether yielded 0.4 g (40%) of α-fluoroacetophenone.

^{1}H NMR (300 MHz, $CDCl_3$): δ (ppm) = 5.53 (d, J = 46.92 Hz, 2H, CH_2F), 7.89 (d, J = 6.5 Hz, 2H, Ar), and 7.50 (d, J = 6.5 Hz, 2H, Ar). ^{13}C NMR (75 MHz, $CDCl_3$): δ (ppm) = 84.2 (d, J = 182.60 Hz, CH_2F), 128.8, 129.9, 135.1, and 194.8 (d, J=15.5 Hz, CO).

p-Methoxy-α-fluoroacetophenone(MFA). The same procedure that was used for the synthesis of α-fluoroacetophenone was followed, but using *p*-anisoyl chloride instead of benzoyl chloride. The pure product was obtained in 44% (0.44 g).

^{1}H NMR (300 MHz, $CDCl_3$): δ (ppm) = 5.47 (d, J = 47.11 Hz, 2H, CH_2F), 7.90 (d, J = 7.1 Hz, 2H, Ar), and 6.96 (d, J = 7.1 Hz, 2H, Ar). ^{13}C NMR (75 MHz, $CDCl_3$): δ (ppm) = 56.09 (OCH_3), 84.2 (d, J = 182.09 Hz, CH_2F), 115.0, 131.3, 165.4, and 193.4 (d, J = 15.5 Hz, CO).

Results and Discussion

Theoretical Calculations. The potential energy surfaces for FA, MFA, and NFA were built for searching the lowest energy structure for each dihedral angle presented in Figure 1. These surfaces presented minimum energy values for 0° and 180° on analyzing ω and φ dihedral angles. Both angles result in the same geometries for FA and NFA, because FA does not have a group at the *para* position, and for NFA because the nitro group is planar to the benzene ring. However, the presence of a methoxyl group, in MFA, led to different geometries for φ = 0° and 180°. Moreover, the ϕ angle is the most important one for the analysis of the conformational behavior of these compounds, and its surface reveal two energy minima at 0° (*cis*) and 150° (*gauche*) for FA, MFA, and NFA (Figure 2).

Thus, as mentioned above, for FA and NFA just the *cis* and *gauche* rotamers were observed (Figure 3), but in the case of MFA, each *cis* and *gauche* form presented two rotamers (*syn* and *anti*) due to methyl position in space, resulting in four conformers in equilibrium (Figure 4).

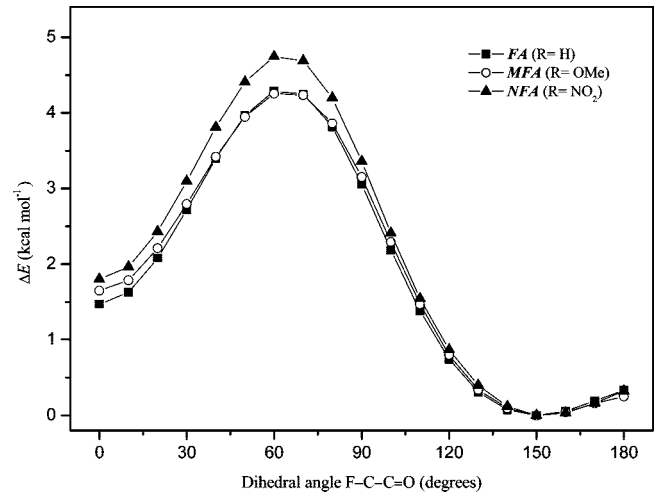

Figure 2. Potential energy surfaces at the B3LYP/6-31g(d,p) level.

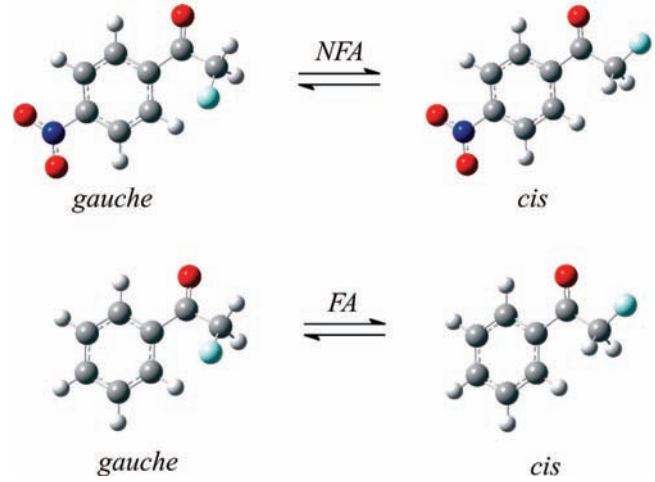

Figure 3. Most stable rotamers for NFA and FA.

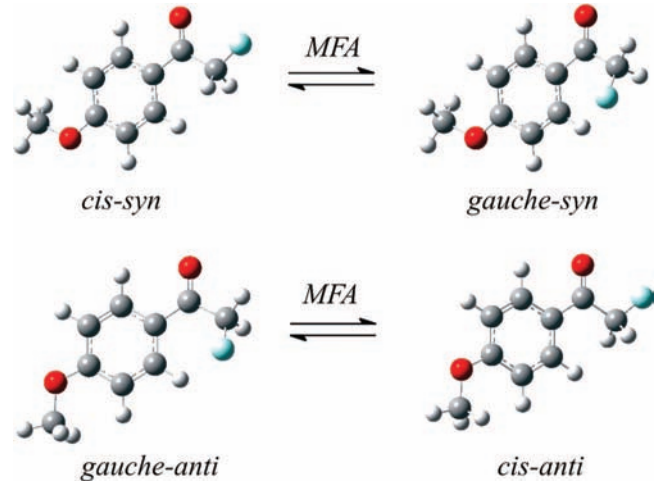

Figure 4. Most stable rotamers for MFA.

The dihedral angles (F−C−C═O) for all *cis* rotamers were 0°. *Gauche* forms were identified through the F−C−C═O dihedral angle of 149.3°, 145.7°, 145.1°, and 148.3° for NFA, FA, MFA-*syn*, and MFA-*anti*, respectively. All geometric parameters, such as bond length, angle, and dihedral angle together with energy, population, and dipole moment to each rotamer are listed in Tables 1 and 2.

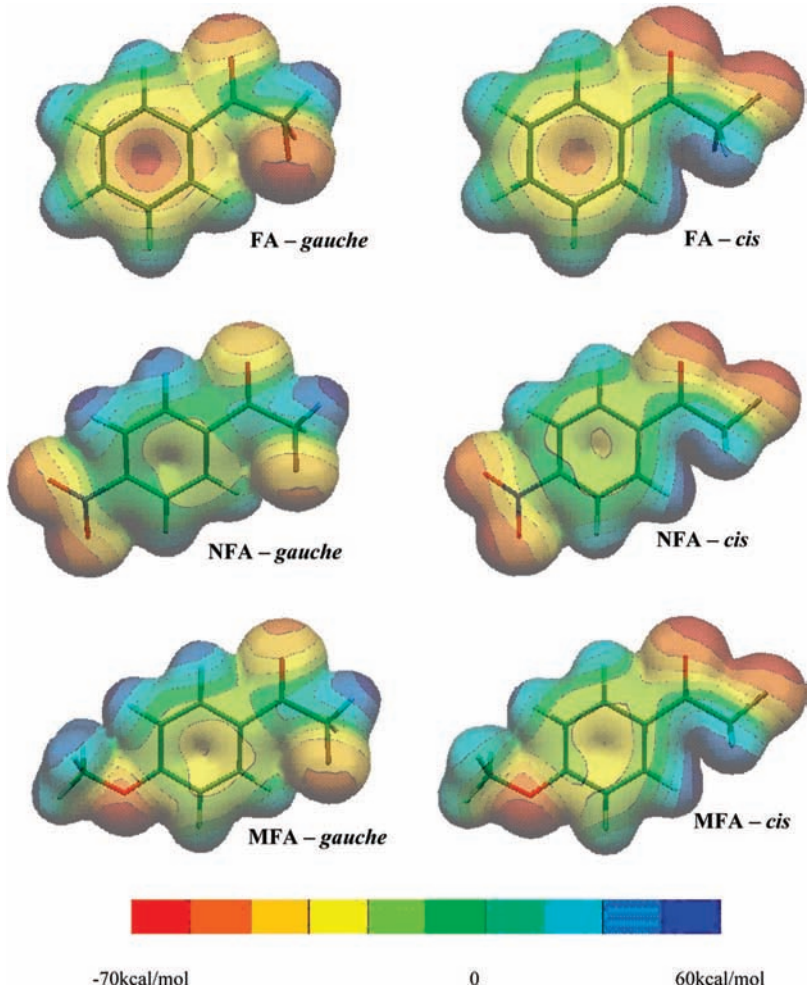

Figure 5. Electrostatic potential maps for FA, NFA, and MFA (0.01 au isodensity surface).

The determination of the conformer populations for FA and NFA were performed by ΔE ($E_{cis} - E_{gauche}$) using the following equations:

$$n_{cis} + n_{gauche} = 1 \quad (1)$$

$$k = \frac{n_{cis}}{n_{gauche}} = \frac{1}{2}\exp^{(\frac{-\Delta E}{RT})} \quad (2)$$

The situation is more complex for MFA, since the four rotamers must be considered—two for the *cis* and two for the *gauche* arrangements—as the methoxyl group has two possible orientations, *syn* and *anti* to the carbonyl group, as follows:

$$n_{cis-anti} + n_{gauche-anti} + n_{cis-syn} + n_{gauche-syn} = 1 \quad (3)$$

$$k_1 = \frac{n_{cis-anti}}{n_{gauche-anti}} = \frac{1}{2}\exp^{(\frac{-\Delta E}{RT})}\, k_2 = \frac{n_{cis-syn}}{n_{gauche-anti}} = \frac{1}{2}\exp^{(\frac{-\Delta E}{RT})}\, k_3 = \frac{n_{gauche-syn}}{n_{gauche-anti}} = \frac{1}{2}\exp^{(\frac{-\Delta E}{RT})} \quad (4)$$

These calculations indicated that the *gauche* form is the most stable for the three compounds. In the *cis* rotamers, the oxygen and fluorine atoms were too close to each other, suggesting a strong electronic repulsion between them. The calculated electrostatic potential maps (Figure 5) clearly show these interactions, identified through the red regions of the maps. Thus, the conformational preference for the *gauche* rotamer can be understood in terms of this electronic repulsion between oxygen and fluorine atoms. This is in agreement with the *gauche* populations from Tables 1 and 2.

NMR Results. The ^{13}C and ^{1}H NMR spectra were recorded in solvents of varying polarity for the three compounds and also for different temperatures for NFA and MFA. Both experiments showed the same behavior. In the former (Table 3), the $^{1}J_{CF}$ values changed from 184.7, 182.6, and 182.1 Hz in $CDCl_3$ to 176.8, 175.6, and 174.8 Hz in DMSO for NFA, FA, and MFA, respectively. The $^{2}J_{C(O)F}$ changed in the same way that $^{1}J_{CF}$ did. These changes in the coupling constants values indicated changes in conformer populations in equilibria.

In an effort to understand the preferences in the conformational equilibrium, the experimental data can be compared to calculated coupling constants (Table 4). Decrease of experimental value of $^{2}J_{C(O)F}$ (Table 3) points out that the conformer with lowest $^{2}J_{C(O)F}$ value (Table 4), the *cis* form, was preferred in relation to the *gauche* form as the solvent polarity increases. The calculated $^{1}J_{CF}$ values were not reported because they do not follow the experimental results.

In the same way, a decrease in the temperature (Table 5 and 6) had the same effect of an increase in solvent polarity (eq 5) and, thus, favoring the *cis* rotamer.

$$\frac{(\varepsilon - 1)(2\varepsilon + 1)}{9\varepsilon} = \frac{n}{\varepsilon_0}\left(\alpha + \frac{\mu^2}{3kT}\right) \quad (5)$$

IR Results. The IR spectra in solvents of varying polarity gave a double band for the carbonyl absorption for the three

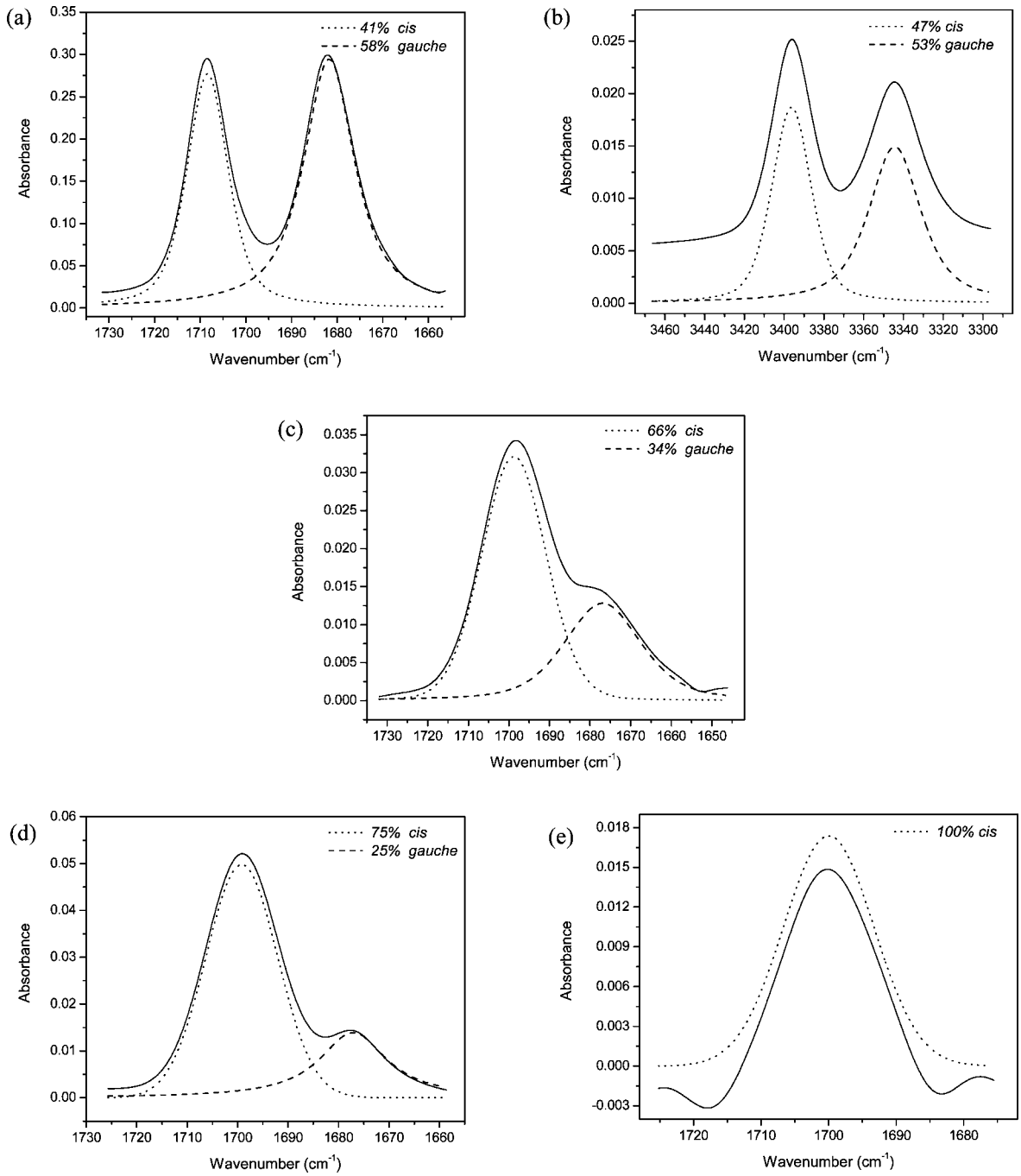

Figure 6. Carbonyl absorption band in the IR spectrum of MFA in (a) CCl_4 and (b) CCl_4, in the first overtone, (c) $CHCl_3$, (d) CH_2Cl_2, and (e) CH_3CN.

TABLE 7: Calculated (Vapor) and Experimental ($CHCl_3$) Infrared Frequencies, in cm^{-1}, for *cis* and *gauche* Rotamers Conformer Population (%) Determined from IR Spectra in CH_3CN ($population_{exp(solvent)}$)[a]

	NFA		FA		MFA	
	cis	*gauche*	*cis*	*gauche*	*cis*	*gauche*
$\nu_{C=Ocalc}$	1773.72	1744.17	1765.52	1732.34	1754.48	1719.72
$\nu_{C=Oexp}$	1719.43	1698.85	1730.09	1706.19	1698.75	1676.90
$population_{exp(solvent)}$	85	15	80	20	100	0
$population_{calc(solvent)}$	84	16	87	13	85	15
$population_{calc(vapor)}$	9	91	14	86	11	89

[a] Calculated populations were done in vapor phase ($population_{calc(vapor)}$) and in CH_3CN ($population_{calc(solvent)}$).

compounds. A deconvolution analysis clearly showed two resolved bands, which confirms the presence of the two rotamers. The band assignments were accomplished by taking into account the calculated frequencies presented in Table 7.

A single band was observed for MFA (Figure 6e) in acetonitrile solution, which indicates just the presence of *cis* conformer (100%) in this solvent. Theoretical calculations showed that in the vapor phase there was 11% *cis*-MFA, but

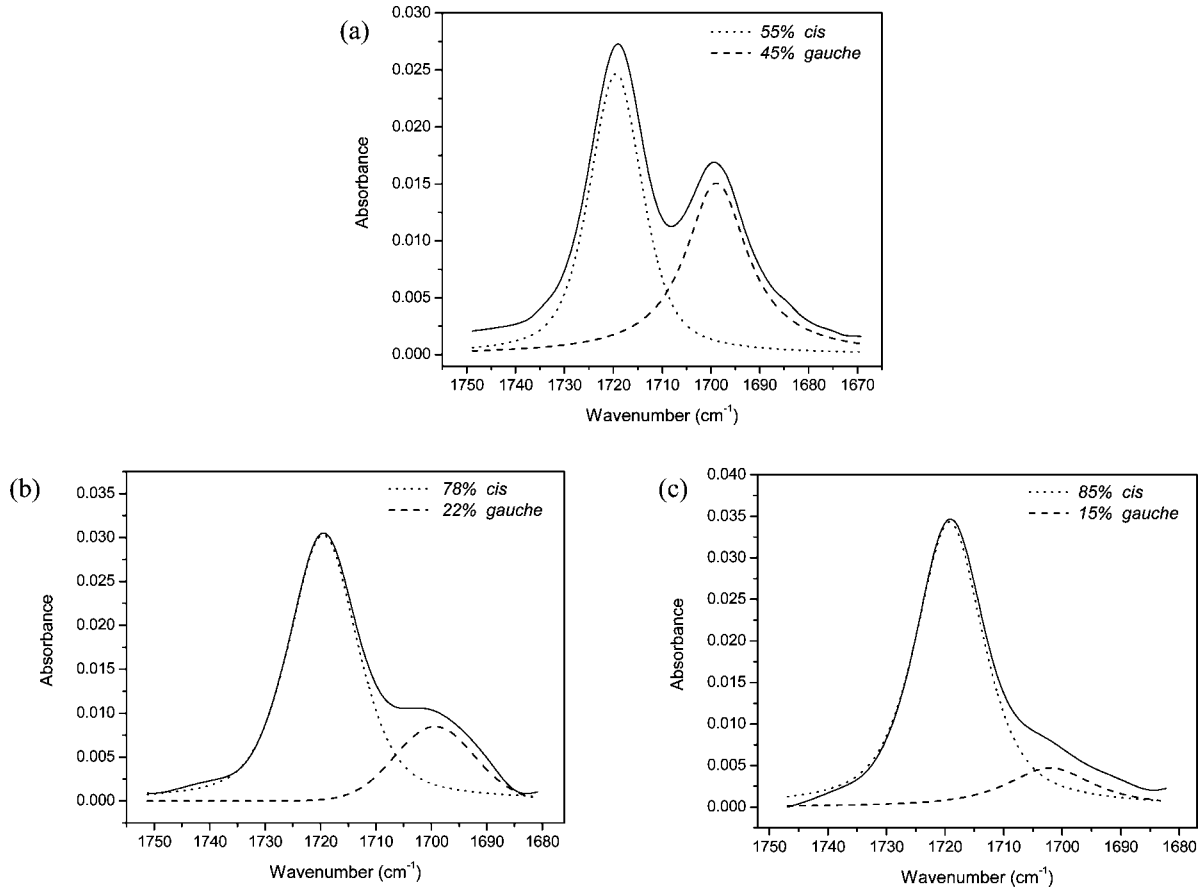

Figure 7. Carbonyl absorption band in the IR spectrum of NFA in (a) $CHCl_3$, (b) CH_2Cl_2, and (c) CH_3CN.

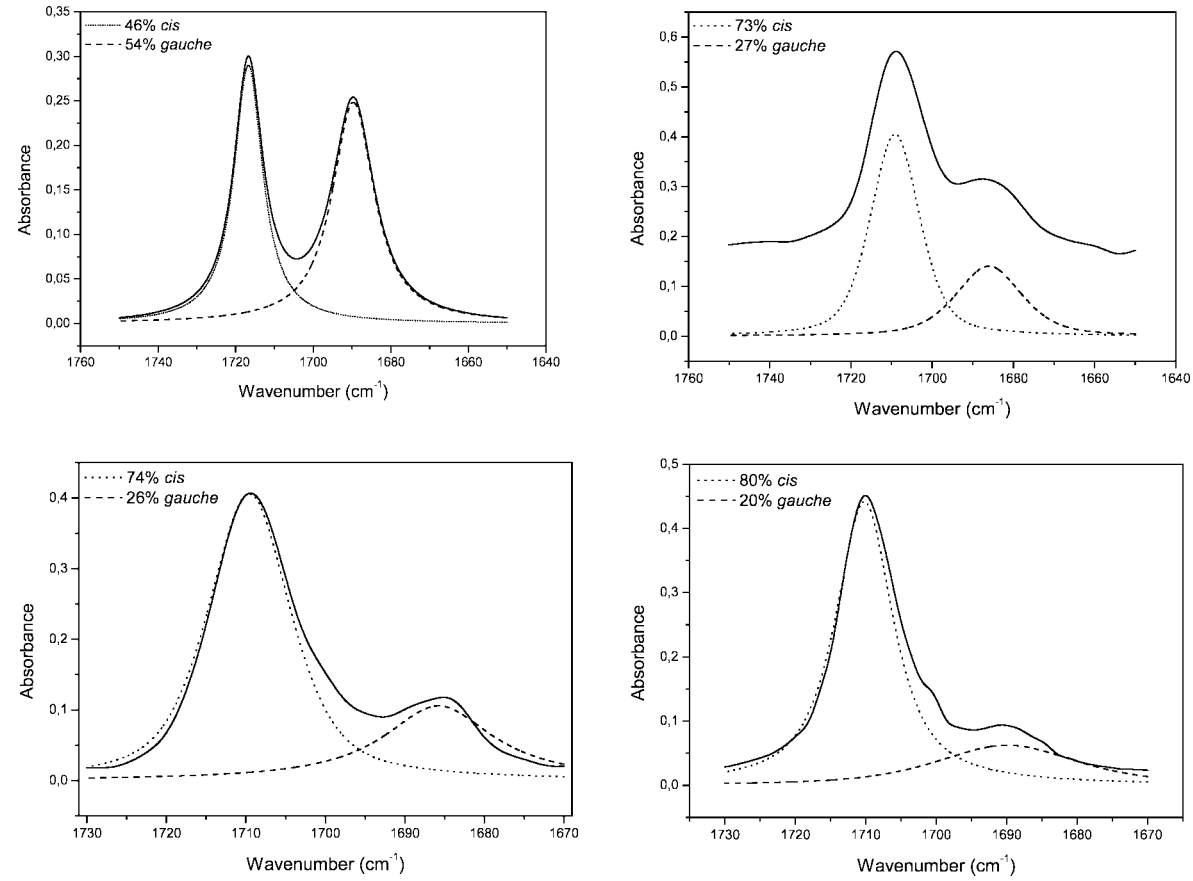

Figure 8. Carbonyl absorption band in the IR spectrum of FA in (a) CCl_4, (b) $CHCl_3$, (c) CH_2Cl_2, and (d) CH_3CN.

85% in acetonitrile solution, while in the other solvents the *cis* population gradually increased as the solvent polarity was increased (Figure 6a−d). Thus, after the inclusion of solvent effects (PCM), the calculated result for acetonitrile solution was in excellent agreement with the experimental one (Table 7).

A similar behavior was observed for NFA and FA (Figures 7 and 8, respectively), where the *cis* population increased when the solvent polarity was gradually increased. Although the calculated population of *cis*-NFA was as little as 9% in the equilibrium, in the vapor phase, the inclusion of solvent effects (acetonitrile) changed that value to 84% (Table 7). This behavior is in good agreement with the observed data in IR experiments, where the *cis*-NFA appears as 55%, 78%, and 85% when the solvent was chloroform, methylene chloride, and acetonitrile, respectively.

The third compound, FA, displayed the same behavior as the other two. The calculated population values for *cis*-FA were 14% (vapor phase) and 87% (acetonitrile) (Table 7), while the experimental values from the IR spectra were 46% (CCl_4), 73% ($CHCl_3$), and 80% (CH_3CN). These data were also corroborated by the NMR experiments.

Conclusions

In summary, it is remarkable that the experimental and theoretical data for the α-fluoroacetophenones are all in full agreement, showing that they present a conformational equilibrium involving the *cis* and *gauche* (∼150°) rotamers. It is also very interesting to note that the occurrence of the *gauche* conformer instead of the *trans*, as observed for most of the α-fluorosubstituted carbonyl compounds, may be due to the fact that the carbonyl group is attached to an aromatic ring, which precludes its interaction with the n_F orbitals. This interaction ($n_F \rightarrow \pi_{CO}^*$) was responsible for the stabilization of the *trans* conformer in α-fluoroacetone[6] and also for the predominance of the *axial* conformer of α-fluorocyclohexanone,[20] both in the vapor phase, while in polar solvents these two compounds showed the same behavior as the α-fluoroacetophenones described in this work. The predominance of the *cis* conformer in polar solvents is usually justified as due to a decrease in the internal electrostatic interactions with the increase in the solvent permittivity.[21]

Acknowledgment. We thank "Centro Nacional de Processamento de Alto Desempenho (CENAPAD-SP)" for computing facilities, FAPESP for financial support (grant no. 2005/59649-0), CAPES for a scholarship (to B.C.F.), and CNPq for fellowships (to R.R. and E.A.B.).

References and Notes

(1) Moss, S. J.; Murphy, C. D.; Hamilton, J. T. G.; McRoberts, W. C.; O'Hagan, D.; Schaffrath, C.; Harper, D. B. *Chem. Commun.* **2000**, 2281.
(2) (a) O'Hagan, D.; Harper, D. B. J. *Fluor. Chem.* **1999**, *100*, 127. (b) Purser, S.; Moore, P. R.; Swallow, S.; Gouverneur, V. *Chem. Soc. Rev.* **2008**, *37*, 320. (c) O'Hagan, D. *Chem. Soc. Rev.* **2008**, *37*, 308.
(3) Phan, H. V.; Durig, J. R. *J. Mol. Struct. (THEOCHEM)* **1990**, *209*, 333.
(4) Pontes, R. M.; Fiorin, B. C.; Basso, E. A. *Chem. Phys. Lett.* **2004**, *395*, 205.
(5) Abraham, R. J.; Tormena, C. F.; Rittner, R. *J. Chem. Soc., Perkin Trans.* **2 1999**, 1663.
(6) Abraham, R. J.; Jones, A. D.; Warne, M. A.; Rittner, R.; Tormena, C. F. *J. Chem. Soc., Perkin Trans. 2* **1996**, 533.
(7) Abraham, R. J.; Tormena, C. F.; Rittner, R. *J. Chem. Soc., Perkin Trans. 2* **2001**, 815.
(8) van der Veken, B. J.; Truyen, S.; Herrebout, W. A.; Watkins, G. *J. Mol. Struct.* **1993**, *293*, 55.
(9) Tormena, C. F.; Rittner, R.; Abraham, R. J.; Basso, E. A.; Pontes, R. M. *J. Chem. Soc., Perkin Trans.* **2 2000**, 2054.
(10) Tormena, C. F.; Amadeu, N. S.; Rittner, R.; Abraham, R. J. *J. Chem. Soc., Perkin Trans. 2* **2002**, 773.
(11) Olivato, P. R.; Guerrero, S.; Hase, Y; Rittner, R. *J. Chem. Soc., Perkin Trans. 2* **1990**, 465.
(12) Catalano, D.; Celebre, G.; Emsley, J. W.; Longeri, M.; Luca, G. D.; Veracini, C. A. *J. Chem. Soc., Perkin Trans. 2* **1998**, 1823.
(13) Rodríguez, A. M.; Giannini, F. A.; Baldoni, H. A.; Santagata, L. N.; Zamora, M. A.; Zacchino, S.; Sosa, C. P.; Enriz, R. D.; Csizmadia, I. G. *J. Mol. Struct.* **1999**, *463*, 271.
(14) Frisch, M. J.; et al. *Gaussian 03*; Gaussian Inc.: Pittsburgh, PA, 2003.
(15) Hehre, W. J. *A Guide to Molecular Mechanics and Quantum Chemical Calculations*; Wavefunction Inc: Irvine, CA, 2003.
(16) Flükiger, P.; Lüthi, H. P.; Portmann, S.; Weber, J. *Molekel 4.3*; Swiss Center for Scientific Computing: Manno, Switzerland; 2000−2002.
(17) Portmann, S.; Lüthi, H. P. *CHIMIA* **2000**, *54*, 766.
(18) Tomasi, J.; Scrocco, E.; Miertus, S. *Chem. Phys.* **1981**, *55*, 117.
(19) Bridge, C. F.; O'Hagan, D. J. *Fluor. Chem.* **1997**, *82*, 21.
(20) Yoshinaga, F.; Tormena, C. F.; Freitas, M. P.; Rittner, R.; Abraham, R. J. *J. Chem. Soc., Perkin Trans. 2* **2002**, 1494.
(21) Eliel, E. L.; Wilen, S. H.; Mander, L. N. *Stereochemistry of Organic Compounds*; Wiley: New York, 1994.

JP808048S